Nuclear matter with chiral forces in Brueckner-Hartree-Fock approximation

Z. H. Li (李增花)[1] and H.-J. Schulze[2]
[1]*Institute of Modern Physics and Applied Ion Beam Physics Laboratory, Key Laboratory of the Ministry of Education, Fudan University, Shanghai 200433, China*
[2]*INFN Sezione di Catania, Dipartimento di Fisica, Via Santa Sofia 64, I-95123 Catania, Italy*
(Received 29 March 2012; revised manuscript received 8 May 2012; published 5 June 2012)

We compute the binding energy of symmetric nuclear matter in the Brueckner-Hartree-Fock approach using chiral two-nucleon and three-nucleon forces. We find strong overbinding, which cannot be remedied by the current version of three-body forces.

DOI: 10.1103/PhysRevC.85.064002 PACS number(s): 21.45.Ff, 21.65.Mn, 24.10.Cn

I. INTRODUCTION

The idealized system of symmetric nuclear matter is a traditional benchmark environment for theoretical many-body methods [1], apart from its practical interest for the physics of heavy-ion collisions and stellar structure, for example. In particular, a realistic reproduction of the empirical saturation point of nuclear matter is already a nontrivial task [2,3]. It is now known that any realistic many-body approach requires as input two-nucleon forces (2NF) supplemented by three-nucleon forces (3NF) in order to achieve this goal.

While several high-quality nucleon-nucleon (NN) potentials are available nowadays, the development of consistent microscopic 3NF is a matter of current research. Traditionally the meson-exchange picture [4] is used to derive or motivate NN potentials and also 3NF. A new development is the derivation of 2NF and 3NF in a low-momentum expansion based on chiral symmetry [5]. So far 2NF have been derived up to fourth order in that manner [6,7], termed N3LO, which allows rather precise fits of the NN phase shifts, at least for not too large scattering energies below about 300 MeV. Chiral 3NF are currently available at N2LO level [8,9], since going to the next order represents still a formidable technical challenge.

It is thus of interest to examine the predictions of the current 2NF (N3LO) + 3NF (N2LO) interaction in combination with a many-body method for dense nuclear matter. In this article we perform this study within the Brueckner-Hartree-Fock (BHF) approach to nuclear matter [10,11].

Nuclear and neutron matter have recently also been studied in a variational method [12], employing the same chiral 3NF, but in combination with the empirical Argonne V_8' potential instead of the consistent chiral 2NF. Few-body calculations of ^{3}H and ^{4}He nuclei with the same 2NF (N3LO) + 3NF (N2LO) chiral interaction have been carried out in [9,13] and with the 2NF (V_{18}) + 3NF (N2LO) interaction in [14].

We remark finally that sometimes the chiral forces are further transformed into effective "low-momentum" interactions [15–17], which simplifies related many- and few-body calculations. This procedure introduces additional assumptions and parameters, and we will make some comparison at the end.

We now briefly review the formalism of treating 3NF within the BHF approach, specify the N2LO 3NF within this method, and then present our results.

II. FORMALISM

We use the N3LO 2NF of Ref. [6], which is in practice given in terms of the usual operator structure of a NN potential in momentum space and can be employed straightforwardly in the Bethe-Goldstone equation (5). It involves a chiral cutoff $\Lambda = 500$ MeV, the same as also applied in the N2LO 3NF later.

At the present state of the art of the BHF approach, the 3NF is reduced to an effective density-dependent local 2NF in coordinate space by averaging over the third nucleon in the medium [18–27], taking account of the NN in-medium correlations by means of the BHF NN correlation function g:

$$\overline{V}_{12}(\boldsymbol{r}) = \overline{\sum_{\sigma_3,\tau_3}}\ \overline{\sum_{r_3}} V_{132} \tag{1}$$

with

$$\overline{\sum_{r_3}} = \rho \int d^3r_3\, g_x^2 g_y^2, \quad \int d^3r_3 = \frac{2\pi}{r}\int_0^\infty dx\, x \int_{|r-x|}^{r+x} dy\, y, \tag{2}$$

and $\boldsymbol{r} = \boldsymbol{r}_2 - \boldsymbol{r}_1$, $\boldsymbol{x} = \boldsymbol{r}_3 - \boldsymbol{r}_1$, $\boldsymbol{y} = \boldsymbol{r}_3 - \boldsymbol{r}_2$. Here the correlation function g is related to the BHF defect function η,

$$g_r = 1 - \eta(r), \ \ \eta(r) = \phi_{LSJ}(kr) - u_{LSJ}(k,r), \tag{3}$$

with the (un)correlated wave functions $(\phi)u$, where in practice only the s waves are considered and a suitable average in momentum space is performed [23–25].

The result is an effective local NN potential with the operator structure

$$\begin{aligned}\overline{V}_{12}(\boldsymbol{r}) = {} & V_I(r) + (\boldsymbol{\sigma}_1\cdot\boldsymbol{\sigma}_2)V_S(r) + (\boldsymbol{\tau}_1\cdot\boldsymbol{\tau}_2)V_N(r)\\ & + (\boldsymbol{\tau}_1\cdot\boldsymbol{\tau}_2)(\boldsymbol{\sigma}_1\cdot\boldsymbol{\sigma}_2)V_C(r)\\ & + S_{12}(\hat{\boldsymbol{r}})[(\boldsymbol{\tau}_1\cdot\boldsymbol{\tau}_2)V_T(r) + V_Q(r)],\end{aligned} \tag{4}$$

where $S_{12}(\hat{\boldsymbol{r}}) = 3(\boldsymbol{\sigma}_1\cdot\hat{\boldsymbol{r}})(\boldsymbol{\sigma}_2\cdot\hat{\boldsymbol{r}}) - \boldsymbol{\sigma}_1\cdot\boldsymbol{\sigma}_2$ is the tensor operator and the components V_O, $O = I, S, N, C, T, Q$ depend on the nucleon density $\rho = 2k_F^3/3\pi^2$. They are added to the bare potential V_{2NF} in the Bethe-Goldstone equation for the G matrix,

$$G[E;\rho] = V + \sum_{k_1,k_2>k_F} V \frac{|k_1k_2\rangle\langle k_1k_2|}{E - e(k_1) - e(k_2) + i\epsilon} G[E;\rho] \tag{5}$$

 ©2012 American Physical Society

with $V = V_{2NF} + V_{3NF}$, and are recalculated together with the single-particle energy $e(k) = k^2/2m_N + U(k)$,

$$U(k;\rho) = \mathrm{Re} \sum_{k' \leqslant k_F} \langle kk'|G[e(k)+e(k');\rho]|kk'\rangle_A, \quad (6)$$

and the defect functions in every BHF iteration step until convergence is reached. In the BHF approximation the energy per nucleon is then given by

$$\frac{B}{A} = \frac{3}{5}\frac{k_F^2}{2m_N} + \frac{1}{2\rho}\mathrm{Re} \sum_{k_1,k_2 \leqslant k_F} \langle k_1k_2|G[e(k_1)+e(k_2);\rho]|k_1k_2\rangle_A. \quad (7)$$

We thus use the standard two-hole line (BHF) approximation with the continuous choice of single-particle energies. It has been confirmed that this is a reliable procedure within the hole-line expansion [11], since the three-hole line contributions have been shown to be quite small [28].

The 3NF averaging procedure avoids the difficult problem of solving the relevant Faddeev equation involving 3NF. It allows us to include the direct and some single-exchange 3NF diagrams in the ladder summation of the BHF approximation, but neglects in particular the double-exchange 3NF diagrams [19–21,23]. The individual sizes of these missing contributions have been estimated to be of the order of 20% [20]. This approximation has been extensively used and considered reliable in the past. Going beyond it will require a consistent inclusion of 3NF into the hole-line expansion, a considerable effort which might be achieved in the future.

Within a meson-exchange approach the different components $V_O(r)$ of the effective 3NF, Eq. (4), are specified in detail in Ref. [26]. The $\pi\pi$ contribution, which appears in equivalent form in the chiral 3NF, reads explicitly in the standard Tucson-Melbourne (TM) notation involving the parameters a, b, c [20,29] (in the following m denotes the pion mass)

$$\begin{aligned} V_O^{\pi\pi}(r) = m\left(\frac{g_{\pi NN}m}{8\pi m_N}\right)^2 \frac{1}{3}\overline{\sum_{r_3}} & \\ \times\bigg[& (a-2c)z_r G_x G_y + c z_r (F_x G_y + F_y G_x) \\ & + \frac{b}{3}(Y_x Y_y + 2P_r T_x T_y)\bigg], (O=C) \\ \times\bigg[& (a-2c)Q G_x G_y + cQ(F_x G_y + F_y G_x) \\ & + \frac{b}{3}(P_x Y_x T_y + P_y Y_y T_x + P T_x T_y)\bigg], (O=T), \end{aligned} \quad (8)$$

while for the N2LO contact-term contributions [12,14] we find the effective averaged potentials

$$\begin{aligned} V_O^D(r) = c_D \left(\frac{m^2}{4\pi F_\pi^2}\right)^2 \frac{m^2}{\Lambda_\chi}\frac{g_A}{8}\frac{1}{3}\overline{\sum_{r_3}} & \\ \times [Y_x Z_y + Y_y Z_x], & (O=C) \\ \times [P_y T_x Z_y + P_x T_y Z_x], & (O=T) \end{aligned} \quad (9)$$

and

$$V_N^E(r) = c_E\left(\frac{m^2}{4\pi F_\pi^2}\right)^2 \frac{m^2}{\Lambda_\chi}\overline{\sum_{r_3}} Z_x Z_y \quad (10)$$

with the following definitions and abbreviations:

$$\begin{aligned} z_r &\equiv \hat{\boldsymbol{x}}\cdot\hat{\boldsymbol{y}} = \frac{x^2+y^2-r^2}{2xy}, \\ z_x &= \frac{r^2+y^2-x^2}{2ry}, \quad z_y = \frac{r^2+x^2-y^2}{2rx}, \quad (11) \\ P_r &\equiv P_2(z_r) = \frac{3z_r^2-1}{2}, \\ Q &= -\frac{z_r+3z_xz_y}{2}, \quad P = 3z_rQ - P_x - P_y. \quad (12) \end{aligned}$$

The various form factor functions F, G, Y, T, Z are defined as

$$Z_r = Z_0(r), \quad (13a)$$

$$F_r = -\frac{1}{m}\frac{\partial}{\partial r}Z_0(r), \quad (13b)$$

$$G_r = -\frac{1}{m}\frac{\partial}{\partial r}Z_1(r), \quad (13c)$$

$$Y_r = \frac{1}{m^2}\left(\frac{\partial^2}{\partial r^2} + \frac{2}{r}\frac{\partial}{\partial r}\right)Z_1(r), \quad (13d)$$

$$T_r = \frac{1}{m^2}\left(\frac{\partial^2}{\partial r^2} - \frac{1}{r}\frac{\partial}{\partial r}\right)Z_1(r), \quad (13e)$$

based on the propagator functions Z_0 and Z_1,

$$\begin{aligned} Z_n(r) &= \frac{4\pi}{m^{(3-2n)}}\int\frac{d^3\boldsymbol{q}}{(2\pi)^3}e^{i\boldsymbol{q}\cdot\boldsymbol{r}}\frac{e^{-q^4/\Lambda^4}}{(\boldsymbol{q}^2+m^2)^n} \quad (14) \\ &= \frac{4\pi}{m^{(3-2n)}}\frac{1}{2\pi^2}\int dq\, q^2 j_0(qr)\frac{e^{-q^4/\Lambda^4}}{(q^2+m^2)^n}, \quad (15) \end{aligned}$$

regulated with the quartic exponential cutoff employed in Refs. [9,12–14]. Figure 1 illustrates the different form factor functions. One notes in particular the small magnitude of

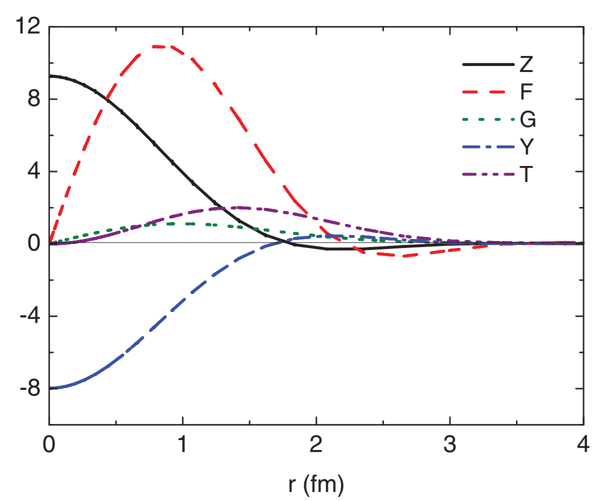

FIG. 1. (Color online) Different form factors, Eq. (13).

the function G, which implies the minor importance of the parameter a (and c) in Eq. (8). Z and Y probe dominantly the short-range part of the nuclear correlations.

The 3NF at N2LO level produces therefore effective contributions in the $O = N, C, T$ channels. A possible ambiguity regarding the N channel ($\sim \boldsymbol{\tau}_1 \cdot \boldsymbol{\tau}_2$) contribution stemming from the E term, Eq. (10), has been discussed in detail in Ref. [12], but this is the operator structure that has also been selected in the few-body calculations of ^{3}H and ^{4}He nuclei [9] that are used to fix some parameters of the model.

In fact the various parameters of the N2LO 3NF are chosen as in [9,12–14], namely we use $m = 138$ MeV, $F_\pi = 92.4$ MeV, $\Lambda = 500$ MeV, $\Lambda_\chi = 700$ MeV, $g_A = 1.29$, and the standard $\pi\pi$ 3NF parameters $c_1 = -0.81$ GeV^{-1} and $c_3 = -3.2$ GeV^{-1} compatible with the N3LO 2NF [5,9]. This yields

$$g_{\pi NN} = \frac{g_A m_N}{F_\pi} \approx 13.10 \tag{16}$$

according to the Goldberger-Treiman relation, and [9]

$$a - 2c = \frac{4m^2}{F_\pi^2} c_1 m \approx -1.00, \tag{17}$$

$$b = \frac{2}{F_\pi^2} c_3 m^3 \approx -1.97, \tag{18}$$

$$c = 0, \tag{19}$$

which is close to the most recent phenomenological meson-exchange parametrization TM99′ [29], $a = -1.12$, $b = -2.80$, $c = 0$ (with different regularization, however). The choice of the contact term parameters c_D and c_E is discussed in the following.

III. RESULTS

In order to illustrate qualitatively the effect of the different components $V_O(r)$ of the averaged 3NF, Eq. (4), we start by setting $c_D = c_E = 1$ and c_1, c_3 as specified above, and display the effective potentials obtained at normal density, $\rho = 0.17$ fm^{-3}, in Fig. 2. For this choice of parameters all

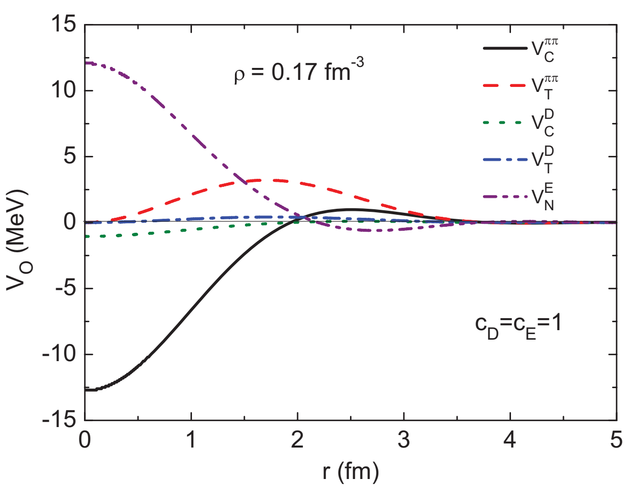

FIG. 2. (Color online) Different components, Eq. (4), of the effective 3NF with $c_D = c_E = 1$ at normal density.

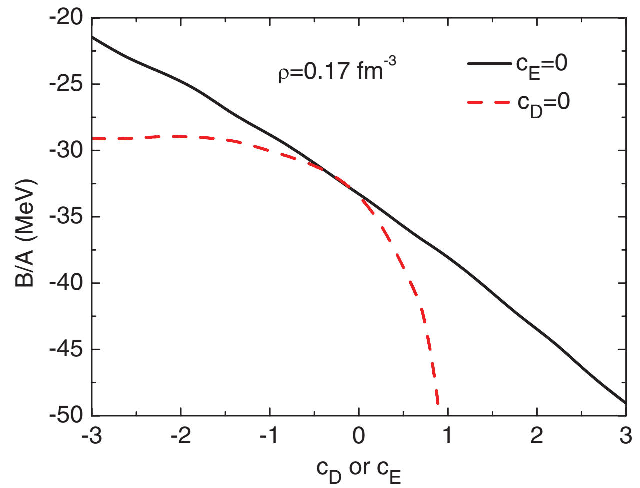

FIG. 3. (Color online) Binding energy of symmetric nuclear matter at normal density as a function of c_D with $c_E = 0$ and vice versa.

components turn out to have an attractive effect in symmetric matter, consistent with the nuclear matter results of Ref. [12]: One observes fairly attractive $\pi\pi$ parts $V_{C,T}^{\pi\pi}$ and also V_N^E corresponds to substantial attraction in symmetric matter, while the $V_{C,T}^D$ components are also very weakly attractive. The qualitative reason for the different magnitudes of the D and E contributions is essentially the global relative factor $g_A/8 \approx 1/6$ in their definition, Eqs. (9), (10).

Since with the N3LO 2NF potential alone symmetric matter at high density is strongly overbound in the BHF approximation (see the solid curve in Fig. 4), it is obvious from this result that at least one of the parameters c_D or c_E has to have a large negative value in order to potentially create the required repulsive effect of the 3NF. We examine this hypothesis in Fig. 3, where the value of the BHF binding energy of symmetric nuclear matter at normal density is shown as a function of c_D for $c_E = 0$ or vice versa. It is, however, obvious from this figure that even for fairly large values of the parameters, a realistic value $B/A \approx -15$ MeV cannot be reached. The main reason is the very attractive $\pi\pi$ force, which causes (with parameters uniquely fixed by the N3LO 2NF) additional binding of the order of 10 MeV at normal density. This in turn is due to the small value of the chiral momentum-space cutoff, which extends the attraction in coordinate space (Fig. 2) up to much larger values ($r \lesssim 2$ fm) than is the case with typical meson-exchange potentials which operate with larger cutoffs; see, e.g., Fig. 1 of [27]. The iteration in the BHF ladder of the averaged $\pi\pi$ 3NF, which has the operator structure of a one-pion-exchange potential, leads then to a fairly strong attraction in symmetric matter.

This is confirmed by Fig. 4 that shows the saturation curves of symmetric nuclear matter up to a density of $\rho = 0.5$ fm^{-3}, which is perhaps at the limit of validity of the chiral N3LO potential, which is more restricted in energy/density than the traditional meson-exchange/phenomenological potentials: The Fermi momentum at this density is about 2 fm^{-1}, similar to the relative momenta for NN scattering at a laboratory energy of 350 MeV. We compare different representative choices of c_D

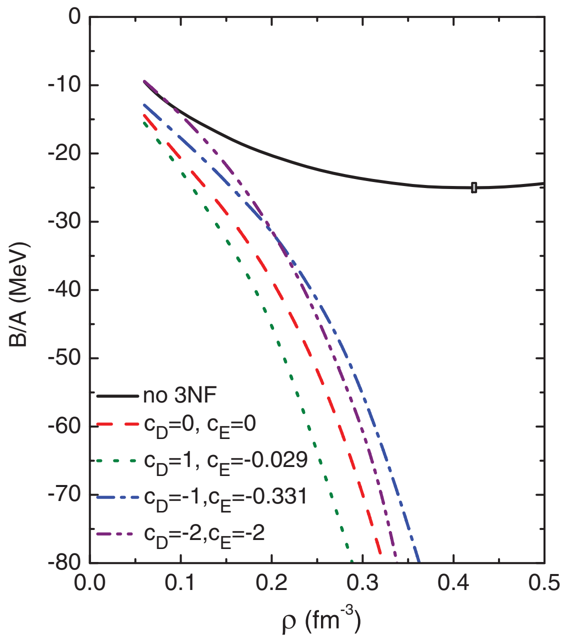

FIG. 4. (Color online) Saturation curves of symmetric nuclear matter with different choices of c_D and c_E. The saturation point without 3NF is indicated on the solid curve.

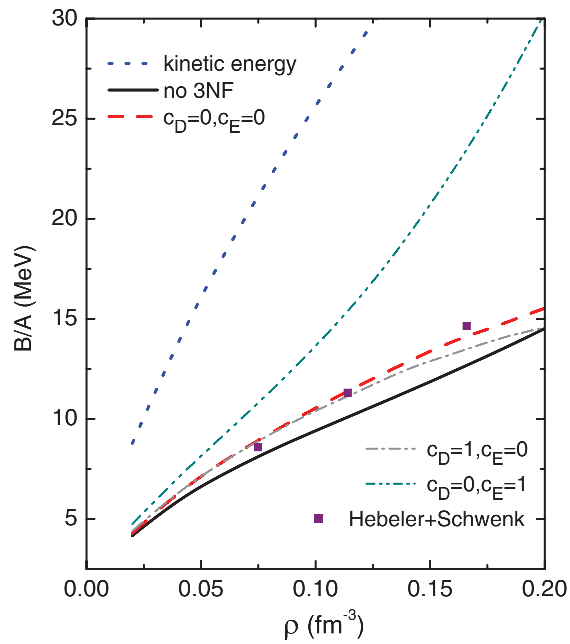

FIG. 5. (Color online) Energy of pure neutron matter in different approximations. The markers represent results of Ref. [16].

and c_E, namely (i) $c_D = c_E = 0$ (red dashed): using only the $\pi\pi$ part of the 3NF; (ii) $c_D = 1$, $c_E = -0.029$ (green dotted): the choice made in Ref. [9] in order to fit the binding energies of ^{3}H and ^{4}He in a no-core shell model; (iii) $c_D = -1$, $c_E = -0.331$ (blue dash-dotted): an alternative choice made in Refs. [9,13] for the same purpose; (iv) $c_D = c_E = -2$ (purple dash-dot-dotted): a supposedly rather repulsive contribution to the 3NF, according to the previous considerations. From the results (in all cases the total 3NF contribution is attractive and no saturation is obtained at all) one can conclude that in the present approximation the main effect of chiral 3NF is provided by the attractive $\pi\pi$ part, which parameters are fixed already at the two-body level. For no choice of the independent additional parameters c_D, c_E satisfactory saturation properties can be obtained in the BHF approximation.

The dominance of the attractive $\pi\pi$ part has also been pointed out in Refs. [9,12,14]. We briefly comment on the related nuclear matter calculations of Refs. [12] and [17]. Both involve exactly the same N2LO 3NF as studied in our work. In the FHNC calculation of [12] this force is combined with the Argonne V_8' 2NF, breaking the consistency of the chiral environment. Nevertheless, also with this combination no satisfactory saturation properties of nuclear matter could be obtained.

In [16] both 2NF and 3NF are further "renormalization-group" transformed to low-momentum forces, effectively removing the short-distance part of the interactions, and allowing a perturbative treatment up to second order. As a consequence the 2NF becomes highly attractive (symmetric matter does not saturate any more) and a large and repulsive 3NF is required in order to restore saturation, which then depends on the various regularization parameters of the model. In this sense this approach is counterintuitive to the meson-exchange picture; see also the extended discussion in [15] and [1].

For completeness we show in Fig. 5 the binding energy of pure neutron matter in our approach. As has been discussed in great detail in Ref. [12], in this environment the D and E contact contributions vanish in the case of the unregularized model with very large cutoff Λ; however, in the case of finite cutoff their contributions can be substantial. This feature may presently be regarded as a conceptual problem of the regularized theory [30]. We therefore present in the figure results with different choices of parameters: The solid black curve shows the N2LO 2NF result without 3NF contribution, and the dashed red curve includes 3NF without contact term contributions, i.e., $c_D = c_E = 0$. In neutron matter the effect of the $\pi\pi$ 3NF is rather small and repulsive, due to the missing $^3SD_1$ tensor force attraction. The BHF result happens to be very close (within 0.5 MeV) to the comparable one of the second-order perturbative calculation with low-momentum interactions of Ref. [16] (markers), even though the in-medium averaging procedure for the 3NF in the latter case allows us to include also the double-exchange diagrams in contrast to the BHF procedure. The effect of the contact terms is demonstrated by the gray dash-dotted ($c_D = 1$, $c_E = 0$) and turquoise dash-dot-dotted ($c_D = 0$, $c_E = 1$) curves. In particular the E contribution is thus potentially substantial [12] and could be used to adjust the neutron matter binding energy. However, in view of the comments above and the results obtained for symmetric matter, this would not be very meaningful.

IV. SUMMARY

In conclusion, symmetric nuclear matter computed using the N3LO 2NF only is strongly overbound in the BHF approach and not only [17]. Adding the $\pi\pi$ part of the N2LO 3NF adds even further attraction. The D, E-contact terms in the present N2LO version of chiral 3NF are too weak and not able to reverse this situation, even deviating substantially from the typical values of the parameters c_D and c_E obtained from fits to properties of light nuclei.

This result is not surprising: It is well known that in the meson-exchange approach to 3NF heavier mesons play a nonnegligible role. In particular, $\pi\rho$ and $\rho\rho$ contributions [21,26] modify strongly (decrease the attraction) the pure $\pi\pi$ part, but only adding scalar contributions [23,24,26,27] allows providing the necessary repulsion required for the saturation mechanism. In the present version of chiral 3NF, these effects of heavier mesons are only partially included in the very rudimentary form of the D, E contact terms. It remains to be seen whether chiral 3NF of higher order are able to provide the missing contributions. Any conclusion based on the current N2LO version of chiral 3NF appears premature.

In the future, apart from developing further the chiral 3NF, it is desirable to set up in particular a consistent treatment of 3NF within the hole-line expansion. However, we do not expect qualitative changes of the results presented here, since the (too) strong attraction of the meson-exchange $\pi\pi$ 3NF has been well known since its invention.

ACKNOWLEDGMENTS

We would like to acknowledge useful correspondence with O. Benhar and A. Kievsky. This work was funded by the National Natural Science Foundation of China under Grant No. 11075037; the Scientific Research Foundation for the Returned Overseas Chinese Scholars, State Education Ministry; the Fundamental Research Funds for the Central Universities of China; the Shanghai Leading Academic Discipline Project (B107); and MIUR PRIN Grant No. 2008KRBZTR.

[1] M. Baldo and G. F. Burgio, Rep. Prog. Phys. **75**, 026301 (2012).
[2] F. Coester, S. Cohen, B. Day, and C. M. Vincent, Phys. Rev. C **1**, 769 (1970); F. Coester, B. Day, and A. Goodman, *ibid.* **5**, 1135 (1972); B. D. Day, Phys. Rev. Lett. **47**, 226 (1981).
[3] Z. H. Li, U. Lombardo, H.-J. Schulze, W. Zuo, L. W. Chen, and H. R. Ma, Phys. Rev. C **74**, 047304 (2006).
[4] R. Machleidt, Adv. Nucl. Phys. **19**, 189 (1989).
[5] R. Machleidt and D. R. Entem, Phys. Rep. **503**, 1 (2011); N. Kalantar-Nayestanaki, E. Epelbaum, J. G. Messchendorp, and A. Nogga, Rep. Prog. Phys. **75**, 016301 (2012).
[6] D. R. Entem and R. Machleidt, Phys. Lett. B **524**, 93 (2002); Phys. Rev. C **68**, 041001(R) (2003).
[7] E. Epelbaum, W. Glöckle, and U.-G. Meissner, Nucl. Phys. A **747**, 362 (2005).
[8] U. van Kolck, Phys. Rev. C **49**, 2932 (1994); E. Epelbaum, A. Nogga, W. Glöckle, H. Kamada, Ulf-G. Meissner, and H. Witała, *ibid.* **66**, 064001 (2002); R. Machleidt and D. R. Entem, J. Phys. G **31**, S1235 (2005); U.-G. Meissner, Eur. Phys. J. A **31**, 397 (2007).
[9] P. Navrátil, Few-Body Systems **41**, 117 (2007).
[10] J. P. Jeukenne, A. Lejeune, and C. Mahaux, Phys. Rep. **25C**, 83 (1976).
[11] M. Baldo, *Nuclear Methods and the Nuclear Equation of State*, International Review of Nuclear Physics, Vol. 8 (World Scientific, Singapore, 1999).
[12] A. Lovato, O. Benhar, S. Fantoni, and K. E. Schmidt, Phys. Rev. C **85**, 024003 (2012).
[13] P. Navrátil, V. G. Gueorguiev, J. P. Vary, W. E. Ormand, and A. Nogga, Phys. Rev. Lett. **99**, 042501 (2007).
[14] A. Kievsky, M. Viviani, L. Girlanda, and L. E. Marcucci, Phys. Rev. C **81**, 044003 (2010).
[15] S. K. Bogner, R. J. Furnstahl, and A. Schwenk, Prog. Part. Nucl. Phys. **65**, 94 (2010).
[16] K. Hebeler and A. Schwenk, Phys. Rev. C **82**, 014314 (2010).
[17] K. Hebeler, S. K. Bogner, R. J. Furnstahl, A. Nogga, and A. Schwenk, Phys. Rev. C **83**, 031301 (2011).
[18] B. A. Loiseau, Y. Nogami, and C. K. Ross, Nucl. Phys. A **165**, 601 (1971).
[19] B. H. J. McKellar and R. Rajaraman, Phys. Rev. C **3**, 1877 (1971); D. W. E. Blatt and B. H. J. McKellar, *ibid.* **11**, 614 (1975).
[20] S. A. Coon, M. D. Scadron, P. C. McNamee, B. R. Barrett, D. W. E. Blatt, and B. H. J. McKellar, Nucl. Phys. A **317**, 242 (1979); S. A. Coon and W. Glöckle, Phys. Rev. C **23**, 1790 (1981).
[21] R. G. Ellis, S. A. Coon, and B. H. J. McKellar, Nucl. Phys. A **438**, 631 (1985); S. A. Coon and M. T. Peña, Phys. Rev. C **48**, 2559 (1993); A. Stadler, J. Adam, H. Henning, and P. U. Sauer, *ibid.* **51**, 2896 (1995); J. Adam, M. T. Peña, and A. Stadler, *ibid.* **69**, 034008 (2004); S. A. Coon, M. T. Peña, and D. O. Riska, *ibid.* **52**, 2925 (1995).
[22] P. Grangé, M. Martzolff, Y. Nogami, D. W. L. Sprung, and C. K. Ross, Phys. Lett. B **60**, 237 (1976); P. Grangé and M. Martzolff, Nuovo Cimento Lett. **16**, 156 (1976); M. Martzolff, B. Loiseau, and P. Grangé, Phys. Lett. B **92**, 46 (1980).
[23] P. Grangé, A. Lejeune, M. Martzolff, and J.-F. Mathiot, Phys. Rev. C **40**, 1040 (1989).
[24] W. Zuo, A. Lejeune, U. Lombardo, and J.-F. Mathiot, Nucl. Phys. A **706**, 418 (2002); Eur. Phys. J. A **14**, 469 (2002).
[25] X. R. Zhou, G. F. Burgio, U. Lombardo, H.-J. Schulze, and W. Zuo, Phys. Rev. C **69**, 018801 (2004).
[26] Z. H. Li, U. Lombardo, H.-J. Schulze, and W. Zuo, Phys. Rev. C **77**, 034316 (2008).
[27] Z. H. Li and H.-J. Schulze, Phys. Rev. C **78**, 028801 (2008).
[28] B. D. Day, Phys. Rev. C **24**, 1203 (1981); H. Q. Song, M. Baldo, G. Giansiracusa, and U. Lombardo, Phys. Rev. Lett. **81**, 1584 (1998); M. Baldo, G. Giansiracusa, U. Lombardo, and H. Q. Song, Phys. Lett. B **473**, 1 (2000); M. Baldo, A. Fiasconaro, H. Q. Song, G. Giansiracusa, and U. Lombardo, Phys. Rev. C **65**, 017303 (2001); R. Sartor, *ibid.* **73**, 034307 (2006).
[29] S. A. Coon and H. K. Han, Few-Body Systems **30**, 131 (2001).
[30] R. Machleidt and D. R. Entem, J. Phys. G **37**, 064041 (2010).